acta physica slovaca vol. 46 No. 1, 25 – 40 February 1996

ORIENTATION DEPENDENCE OF THE OPTICAL MODEL POTENTIAL FOR LIGHT NUCLEI

M.Y.M. Hassan, H.M.M. Mansour, Z. Metawei
Physics Department, Faculty of Science, Cairo University, Giza, Egypt

Received 4 April 1995, accepted 26 December 1995

Within the optical model potential introduced by Townsend the orientation dependence of the interaction is studied for light nuclei. The elastic scattering differential cross-section and the reaction cross-section are calculated using this interaction potential for ^{12}C - ^{12}C system and ^{16}O - ^{12}C system. Deformed harmonic oscillator charge densities with quadrupole deformations are utilized. Comparison with other theoretical calculations are presented and discussed.

1. Introduction

The optical model potential between two nuclei serves as a basic theoretical tool in describing elastic scattering as well as more complicated nuclear reactions. The most famous methods for calculating the optical potential are, the phenomenological Woods-Saxon, the proximity, the energy density and the double folding model.

Wilson and Townsend [1] derived an approximate optical model scattering series based upon the exact nucleus-nucleus multiple scattering series which had been developed by Wilson [2]. The double folding optical potential is obtained by folding the energy dependent free nucleon-nucleon interaction with the densities for both projectile and target. This formulation is fully energy dependent. It includes the effect of the finite nuclear force, and treats Pauli correlations in an approximate way. This optical potential was used in the context of the eikonal phase shift and neglecting the Pauli correlation effect in the calculations of the elastic scattering, the reaction and the total cross-sections for ^{12}C - ^{12}C system at energies from 200 to 290 MeV [3]. The minor disagreement between theory and experiment was attributed to uncertainties in the real part of the forward neutron-proton scattering amplitude. The remaining discrepancies were attributed to the negligence of the Fermi motion, the off shell effects and the Pauli correlations. However, limiting the experimental slope parameter values to those appropriate to diffractive scattering, has improved the agreement between the theoretical calculation and the experimental data. This showed the validity of the eikonal expansion at such low energy. The elastic scattering for ^{12}C - ^{12}C system was studied by different methods and at different values of energy. The McIntyre [4] parametrization of a phase shift analysis performed on high energy heavy ion elastic scattering was used to investigate ^{12}C - ^{12}C elastic scattering. This fundamental parametrization of the S-matrix elements provided also a realistic analytical deflection function and allowed the nuclear rainbow angle observed in alpha- and heavy-ion elastic scattering to be determined accurately.

The ^{12}C - ^{12}C system was investigated also using a double folded potential based on the density and energy dependent DDM3Y interaction [5]. This model was used to investigate 13 sets of elastic scattering data for the systems ^{12}C - ^{12}C, ^{13}C - ^{12}C and ^{16}O - ^{12}C, at laboratory energies between 9 and 120 MeV/nucleon. The density dependent DDM3Y interaction is a modification of the M3Y interaction, to include the density dependence specially at high energy [6]. It is well known that the origin of the density dependence of the effective interaction comes mainly from the Pauli principle effect in the overlapping region and from the energy denominator of the Bethe-Goldstone equation [7]. In this model Brandon and Satchler [5] used a complex potential consisting of a real part calculated by folding the densities with DDM3Y interaction and a phenomenological imaginary part of a Woods-Saxon shape. Good fit was obtained at all energies using this 4-parameter model even though the quality of these fits is not quite as good as could be obtained with 6-parameter Woods-Saxon shaped potential. The energy and density effective interaction was also used to investigate the ^{16}O - ^{12}C system by Kobos et al. [8] and Roussel et al. [9]. Kobos et al. explored a significant modification to the DDM3Y folded potential for obtaining the best fit. They verified that the coupling to the 2^+ state of ^{12}C could be reproduced quite accurately by small change ($\approx 5\%$) in the strength of the absorptive potential.

The complex reaction matrix [10-12] was also used to investigate the ^{12}C - ^{12}C system at $E/A = 85$ MeV. The collective surface vibrational states were included in these calculations, which improved the agreement with the experimental data. A negative sign was obtained for the deformation parameter B_{20}, which reflects the fact that ^{12}C nucleus has an oblate shape. Faessler et al. [12] have investigated ^{12}C - ^{12}C system at energies 1016, 1440 and 2400 MeV, considering the real and imaginary parts of the optical potential between two nuclei calculated in the energy density formalism and the coupling to the collective states was included. They derived the energy density from the Dirac-Brueckner approach to nuclear matter. Ohtsuka [12,13], furthermore, shoved that when the relativistic features are incorporated in the Dirac-Brueckner approach they make the real part of the optical potential less attractive than that obtained in a non-relativistic calculations [13], while the imaginary part was enhanced. The comparison of these results with experimental data showed that the enhancement of the imaginary part in the optical potential improved the agreement with the experimental data, whereas the repulsive contribution to the real part is unfavourable to explain the experimental cross-section. Another method based on the Glauber theory or its "optical limit" was used for the calculation of the ^{12}C - ^{12}C, ^{16}O - ^{12}C elastic scattering. J.Chauvin et al. [14] extended Karol's model [15] to describe the elastic scattering of ^{12}C - ^{12}C at energies 300, 360 and 1016 MeV. This model depends on the experimental nucleon-nucleon forward scattering amplitude and a Gaussian density for both target and projectile nuclei. They found that the final formulation of the model is equivalent

to the optical limit of the Glauber approximation. Their simple calculations gave good agreement with the experimental data at small angles. Also ^{12}C - ^{12}C reaction at 1016 MeV was analyzed [16] using the optical and Glauber models. The analysis shoved that the reaction cross-section in ion-ion scattering in this intermediate energy region is much smaller than that at lower energies. Consequently, the ion makes a much closer approach than that at lower energies and the data provide more detailed information on the nuclear structure and reaction mechanism. At nucleon energies [14, 16] of about 85 MeV/nucleon, the nuclei increase the overlapping and Pauli correlations become important. Using the optical limit of the Glauber theory, Lenzi et al. [17] calculated the elastic and inelastic scattering in terms of eikonal approach, for a variety of colliding nuclei ($4 \leq A_P \leq 40$, $12 \leq A_T \leq 208$) at energy ($E/A_P = 30 - 350$ MeV). They obtained a disagreement between experimental data and the theoretical calculations at large angles for reactions involving ^{12}C nucleus. This disagreement was attributed to the increase in the nuclear transparency. They found that although the eikonal approximation becomes more and more precise at higher energies, the larger transparency increases the sensitivity to the internal part of the nuclear couplings. In this situation a coupled-channel treatment would be more adequate. The most accurate reaction calculations would use the coupled-channels formalism, and include all states populated in the collision. Such a calculation would be very expensive in terms of computer time and memory, and thus it is necessary to simplify the calculation in some manner. So, in the present work the coupling to the 2^+ excited state is included by considering the interacting nuclei as deformed nuclei. We calculate the elastic scattering differential cross-section and the reaction cross-section for ^{12}C - ^{12}C system at energies 1016, 1440 and 2400 MeV. Also, these calculations are performed for ^{16}O - ^{12}C system at energy 1503 MeV. We used the optical potential derived by Wilson [1] including the Pauli correlation effect in the context of the eikonal approximation. Deformed matter densities with static quadrupole deformations are utilized. In section 2, we summarize the formalism used, extending that given by Greiner [ref. 18], Wilson [ref.19], and Hefter [ref. 20]. The calculations and discussion of the results are presented in section 3. Section 4 is devoted to the conclusion.

2. The Formalism

2.1. The Folding Potential for Deformed Nuclei

The nucleus-nucleus optical potential as derived by Wilson takes the form [1]

$$W(r) = A_P A_T \int d^3 r_T \rho_T(r_T) \int d^3 y \rho_P(r + y + r_T) t(e, y)[1 - c(y)] \qquad (2.1)$$

where A_i $(i = P, T)$ are the mass numbers of the projectile and target, ρ_i are the ground state single particle nuclear densities for the colliding nuclei; $t(e, y)$ is the energy dependent constituent-averaged two-nucleon transition amplitude obtained from scattering experiments, e is the $N\bar{N}$ kinetic energy in the c.m. frame, y is the $N\bar{N}$ relative separation and $c(y)$ is the Pauli correlation function, given by

$$c(y) \approx \frac{1}{4}\exp(-k_F^2 y^2/10) \quad \text{and} \quad k_F = 1.36 \ \text{fm} \tag{2.2}$$

This six dimensional integral (2.1) is calculated for deformed nuclei using the momentum space method as derived by Walter Greiner [ref. 18]. If the Fourier transform of a function $f(\bar{x})$ is denoted by $\tilde{f}(\bar{k})$, the folded potential is given by:

$$W(r) = (2\pi)^{-3} \int d^3k \exp[-i\bar{k}\bar{r}]\tilde{\rho}_P(+\bar{k})\tilde{\rho}_T(-\bar{k})t'(e,\bar{k}) \tag{2.3}$$

where

$$t'(e,y) = t(e,y)[1 - c(y)]$$

i.e. the Fourier transformed integrand reduces to a product of the Fourier transforms of the two densities and the transition nucleon-nucleon scattering amplitude. The two nuclei are considered to have a static quadrupole deformation. Following the same steps and notations as in Ref. [18], one can obtain $W(r, \beta_1, \beta_2)$ as follows:

$$W = \sum_{l_1, l_2} W(l_1, l_2)$$

where

$$\begin{aligned} W(0,0) &= \frac{2}{\pi}\int_0^\infty dkk^2 j_0(kr)\tilde{t}'(e,k)A'^{(1)}_{00}(k)A'^{(2)}_{00}(k), \\ W(0,2) &= \frac{2\sqrt{5}}{\pi}\int_0^\infty dkk^2 j_2(kr)\tilde{t}'(e,k)[A'^{(1)}_{00}(k)A'^{(2)}_{20}(k)P_2(\cos\beta_2) + \\ &\quad A'^{(1)}_{20}(k)A'^{(2)}_{00}(k)P_2(\cos\beta_1)], \\ W(2,2) &= \sum_{l=0,2,4} \frac{10}{\pi} i^{-l}(2l+1)\begin{pmatrix} 2 & 2 & l \\ 0 & 0 & 0 \end{pmatrix} \\ &\times \int_0^\infty dkk^2 j_l(kr)\tilde{t}'(e,k)A'^{(1)}_{20}(k)A'^{(2)}_{20}(k) \\ &\times \sum_{m=-2}^{2} \begin{pmatrix} 2 & 2 & l \\ m & -m & 0 \end{pmatrix} d^2_{m0}(\beta_1)d^2_{-m0}(\beta_2) \end{aligned} \tag{2.4}$$

and

$$A'_{ln}(k) = \delta_{n0}\int_0^\infty dr' r'^2 \rho_{l0}(r')j_l(kr'). \tag{2.5}$$

β_1, β_2 are the two Euler angles.

Using equation (2.4) we can calculate the components of the optical potential $W(l_1, l_2)$.

2.2. The Elastic Scattering Differential Cross-Section

The elastic scattering differential cross-section for symmetric system ($^{12}C - ^{12}C$) is given by

$$\sigma_{el} = |f(\Theta) + f(\pi - \Theta)|^2, \tag{2.6}$$

while for the non-symmetric system ($^{16}O - ^{12}C$ is given by

$$\sigma_{el} = |f(\Theta)|^2 \tag{2.7}$$

The elastic scattering amplitude considering the coulomb effect is given by

$$f(\Theta) = f_c(\Theta) + (2ik)^{-1}\sum_l (2l+1)\exp(2i\eta_l)(S_l - 1)P_l(\cos\Theta), \tag{2.8}$$

$f_c(\Theta)$ is the usual point charge Coulomb amplitude, η_l is the point charge Coulomb scattering phase shift, and S_l is given by

$$S_l = \exp(2i\delta_l) \tag{2.9}$$

where δ_l is the complex nuclear phase shift, which are obtained from [19]

$$\delta_l = \frac{1}{2}\chi(b)$$

$$\chi(b) = -\frac{1}{2k}\int_{-\infty}^{\infty} U(b,Z)dZ \tag{2.10}$$

with

$$U(b,Z) = [2mA_P A_T(A_P + A_T)^{-1}]W(b,Z) \tag{2.11}$$

k is incident wave number and $W(b, Z)$ is the optical potential.

2.3. The Density Parameters

We assumed that the intrinsic charge distribution can be described in the form [21]

$$\rho(r) = \rho_0\left(1 + \alpha\left(\frac{r}{a}\right)^2\right)\exp(-r^2/a^2). \tag{2.12}$$

The constant ρ_0 is determined by the normalization condition

$$\int \rho(\bar{r})d\bar{r} = 1, \tag{2.13}$$

and the parameters a and α are taken from Ref. [21].

The density of a nucleus with an axially symmetric deformation, may be written as [20]

$$\rho(r) = \rho_{00}(r) - r\frac{d\rho_{00}(r)}{dr}\sum_l B_{l0}Y_{l0}(\Theta,\phi) \tag{2.14}$$

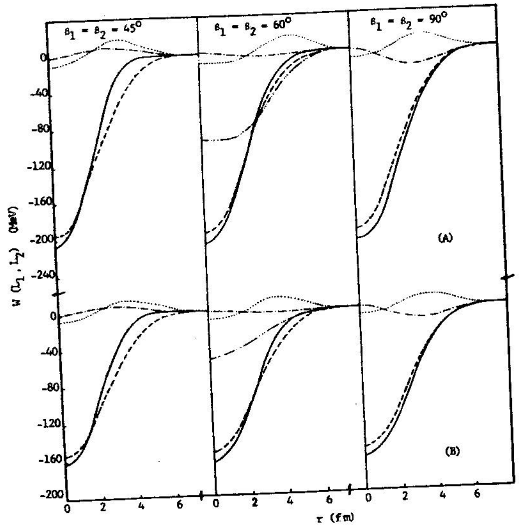

Fig. 1 The real (a) and the imaginary (b) parts of the dominant multipole components of the optical potential for three sets of orientation angle calculated for ^{12}C - ^{12}C at 1016 MeV. The dashed line represents the monopole-monopole force. The dashed dotted line represents the monopole-quadrupole force. The dotted line represents the quadrupole-quadrupole force. The solid line represents the sums over all components. The dashed double dotted line represents Faessler calculations [13].

where $\rho_{00}(r)$ parametrizes the spherical part of the nucleus and B_{l0} is the deformation parameter of the nucleus matter distribution. To calculate the deformation parameter B_{20}, let us consider the transition density

$$\rho_{tr}(r) = B_{l0} r^{l-1} \frac{d\rho_{00}(r)}{dr}. \quad (2.15)$$

The normalization constant B_{20} is determined by assuming that the proton transition density is (Z/A) times the mass transition density and choosing B_{20} to give the measured value of $B(E2)$ for the given nucleus [22], i.e.

$$\int A\rho_{tr}(r) r^{l+2} dr = (A/Ze)(B(El))^{1/2}, \quad (2.16)$$

where A and Z are the mass number and the charge number. The nuclei considered in this work are ^{12}C and ^{16}O. The measured values of $B(E2)$, for these nuclei are

$$B(E2) = 42e^2 \ \text{fm}^4, \quad \text{for} \quad ^{12}\text{C},$$

and

$$B(E2) = 2.15e^2 \ \text{fm}^4, \quad \text{for} \quad ^{16}\text{O}.$$

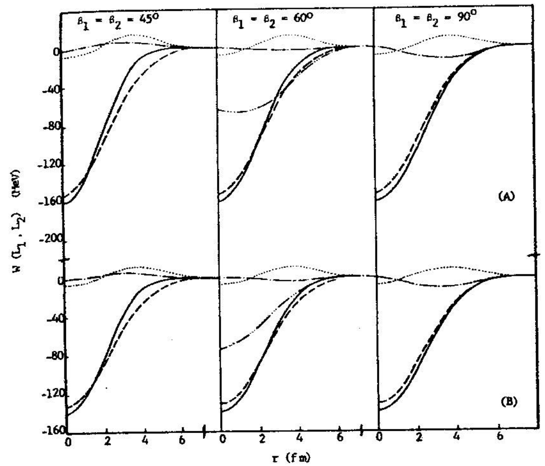

Fig. 2 Same as Fig. 1 but for ^{12}C - ^{12}C at energy 1440 MeV.

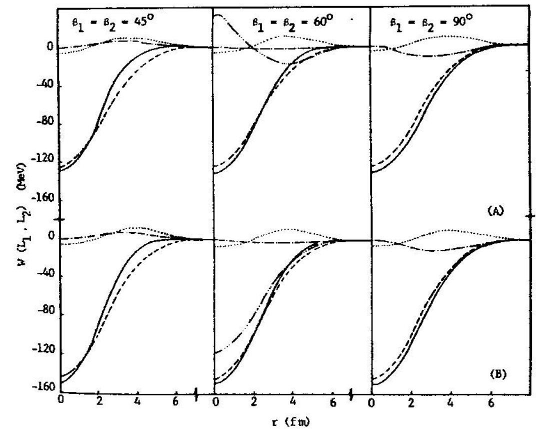

Fig. 3 Same as Fig. 1 but for ^{12}C - ^{12}C at energy 2400 MeV.

3. Results and Discussion

3.1. The Optical Potential

The optical potential between two nuclei at distance r is calculated for ^{12}C - ^{12}C system at E_{lab} = 1016, 1440 and 2400 MeV. Also, the optical potential is calculated for

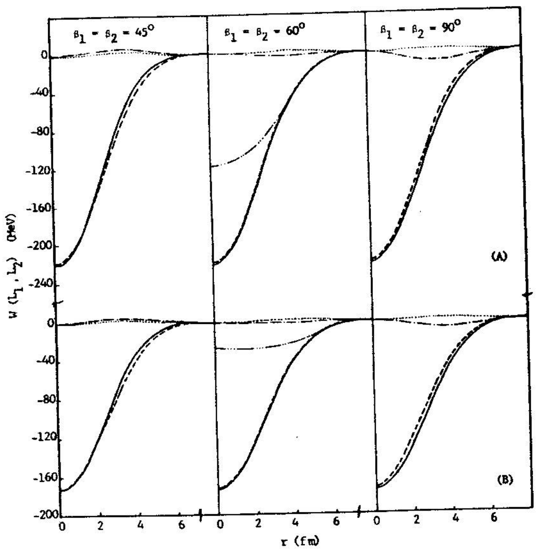

Fig. 4 Same as Fig. 1 but for ^{16}O - ^{12}C at energy 1503 MeV and the dashed double dotted line represents phenomenological potential [23].

Reaction	Energy (MeV)	σ_R (mb)					Ref.
		$\beta_1 = \beta_2$			Experimental results	Other theor. calculations	
		45°	60°	90°			
$^{12}C - ^{12}C$	1016	764.81	1057.10	1291.5	996^{+50}_{-250} 960 ± 25	1040	24
$^{12}C - ^{12}C$	1440	721.53	982.01	1203.1		907 ± 50	25
$^{12}C - ^{12}C$	2400	700.19	945.57	1159.6	860 ± 40	806^{+30}_{-10}	25
$^{16}O - ^{12}C$	1503	1075.90	1221.30	1343.8		1259 1184 1136	9

Table 1 The nucleus-nucleus reaction cross-section compared with other calculated results and with experimental data.

^{16}O - ^{12}C system at energy 1503 MeV. These calculations are performed using equation (2.4) and considering the nucleon-nucleon scattering amplitude $t(e,y)$ to be [1]

$$t(e,y) = -\left(\frac{e}{m}\right)^{1/2} \frac{\sigma(\alpha + i)}{(2\pi\beta)^{3/2}} \exp(-y^2/2B) \tag{3.1}$$

where σ is the average nucleon-nucleon total cross-section, α is the average of the ratio of the real to the imaginary part of the NN forward scattering amplitude and B is the average slope parameter. Figs. 1-4 show the real and the imaginary parts of the dominant components of the optical potential, which are plotted for three sets of

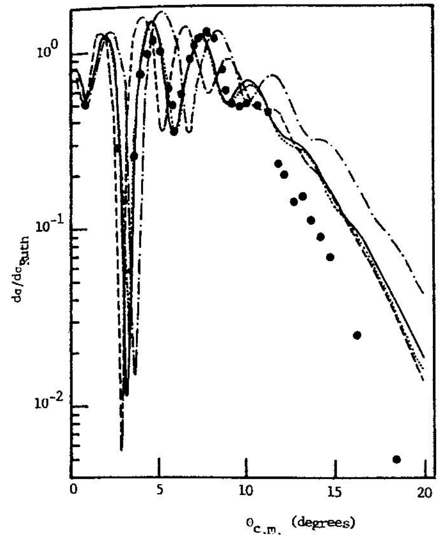

Fig. 5 The elastic scattering differential cross-section calculated for $^{12}C - ^{12}C$ at 1016 MeV for three sets of orientation angles and compared with the results due to monopole-monopole force only. The solid line represents the calculations for $\beta_1 = \beta_2 = 60°$. The dashed line represents the calculations for $\beta_1 = \beta_2 = 90°$. The dashed dotted line represents the calculations for $\beta_1 = \beta_2 = 45°$. The dotted line represents the calculations for the monopole-monopole force.

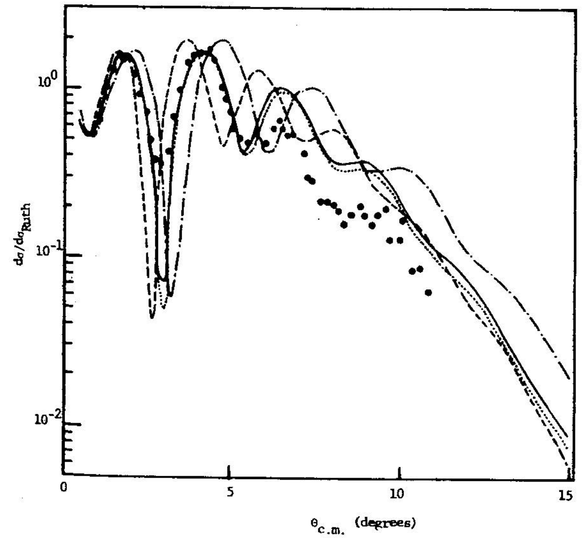

Fig. 6 Same as Fig. 5 but for ^{12}C - ^{12}C at energy 1440 MeV.

the orientation angles $\beta_1 = \beta_2 = 45°, 60°, 90°$. Also, the sums over all components are plotted for each orientation angle. Figs. 1-3 show the optical potential and the dominant

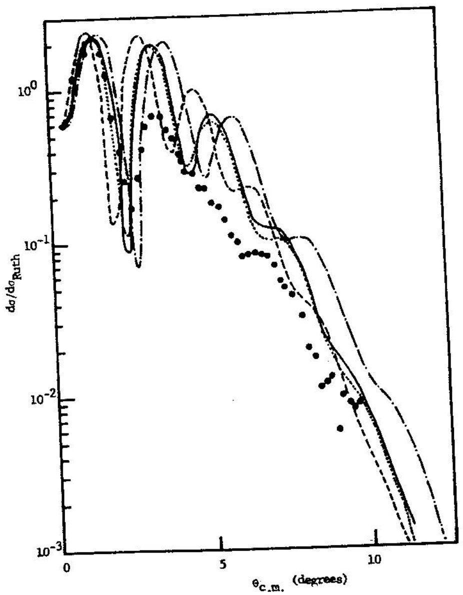

Fig. 7 Same as Fig. 5 but for ^{12}C - ^{12}C at energy 2400 MeV.

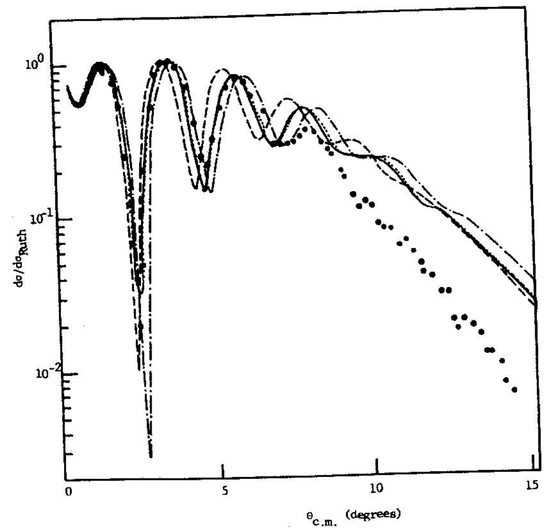

Fig. 8 Same as Fig. 5 but for ^{16}O - ^{12}C at energy 1503 MeV.

components for ^{12}C - ^{12}C reaction at energies 1016, 1440 and 2400 MeV, respectively. Our calculations are compared with those calculated by Faessler [13] using the energy density formalism, and the comparison is made for $\beta_1 = \beta_2 = 60°$. The monopole-

monopole component $W(0,0)$ dominates the contributions for the three orientation angles considered here. The quadrupole-quadrupole component $W(2,2)$ has an opposite sign to the monopole-monopole force at $r \geq 2$. The monopole-quadrupole force has an opposite sign to the monopole-monopole force at $\beta_1 = \beta_2 = 45°$, then it reflects its sign for $\beta_1 = \beta_2 = 60°, 90°$. We can see from these figures that the depth of the optical potential becomes deeper on summing the various components for the three orientations. Also, the depth of the potential is of the same value for the three orientations at definite value of energy. It is clear that the radius of the optical potential increases by increasing the orientation angles. Comparing our potential with the potential calculated by Faessler, one can see that our real and imaginary potentials are deeper, but the two potentials have nearly the same radius. One can see from Fig. 3 that the optical potential calculated by Faessler [13] has positive value at $r = 0$ and changes to a negative value at $r > 2$ and it coincides with our monopole-monopole potential at $r \geq 5$. From Fig. 3, also, it is clear that the imaginary potential has deeper values than the real potential, which is confirmed by the other potential [13]. Comparing the depth of the total optical potential for the three energies considered here, we find that the depth of the real potential is lowered on increasing energy, which is in agreement with the results obtained by Faessler [10, 12, 13]. Fig. 4 shows the real and the imaginary parts of the dominant components and the total optical potential for ^{16}O - ^{12}C reaction at 1503 MeV. Also, the phenomenological [23] potential is presented for comparison with our results. One can see in this figure that the depth of the folding potential is not affected by the monopole-quadrupole and the quadrupole-quadrupole components for any orientation. Comparing our potential with the phenomenological potential, we find that our potential is deeper, but they have the same value as the phenomenological potential in the region $r = 4 - 8$.

3.2. The Elastic Scattering Differential Cross-Section

The elastic scattering differential cross-section is calculated for the reactions under consideration taking into account the excitation of the low-lying collective 2^+ (4.44 MeV) state. Here we calculate the elastic ^{12}C - ^{12}C scattering cross-section at E_{lab} = 1016, 1440 and 2400 MeV using the optical potential obtained in the previous subsection. Also, the elastic scattering for ^{16}O - ^{12}C system is calculated at energy 1503 MeV. Fig. 5 shows the ratios of the elastic cross-section to the Rutherford cross-section for ^{12}C - ^{12}C system at 1016 MeV which is compared with experimental data [24]. These ratios are plotted for three orientation angles $\beta_1 = \beta_2 = 45°, 60°, 90°$ and compared with the theoretical results considering only the monopole-monopole force of the optical potential. One can notice from this figure that the calculated results with orientation angles $\beta_1 = \beta_2 = 45°, 90°$ do not predict the experimental minima and maxima. Our calculations for $\beta_1 = \beta_2 = 90°$ are shifted toward smaller angles and our calculations for $\beta_1 = \beta_2 = 45°$ are shifted towards large angles. The calculated results with orientation angles $\beta_1 = \beta_2 = 60°$ nearly agree with those obtained considering only the monopole-monopole force of the optical potential and give good agreement with experimental data at small angles up to $\Theta_{c.m} = 9°$. These calculated results with $\beta_1 = \beta_2 = 60°$ give the position of the fourth maximum. We can see that our results are larger than the

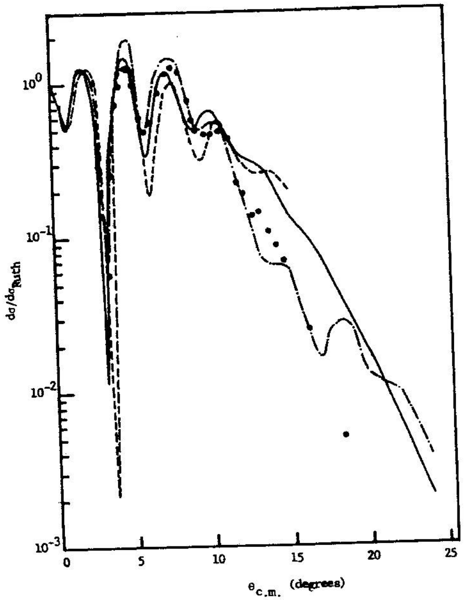

Fig. 9 The elastic scattering differential cross-section of $^{12}C-^{12}C$ at 1016 MeV calculated for $\beta_1 = \beta_2 = 60°$ (solid-line) and compared with the results of Faessler [13] (dashed dotted line) and Lenzi [17] (dashed line).

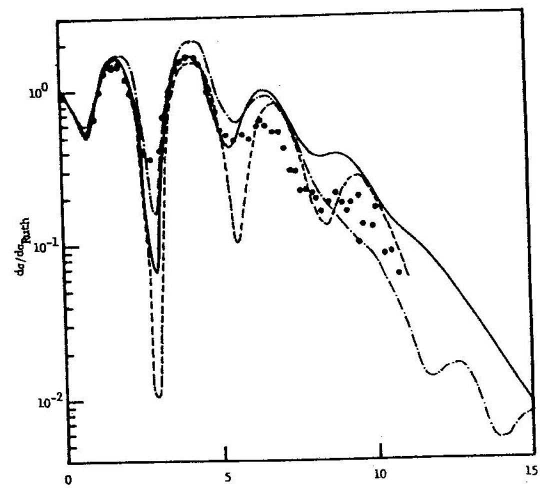

Fig. 10 Same as Fig. 9 but for $^{12}C-^{12}C$ at energy 1440 MeV.

experimental data at the fourth maximum and beyond it. Fig. 6 is the same as Fig. 5 but for $^{12}C-^{12}C$ at 1440 MeV. Also, the experimental data [25] are presented with the

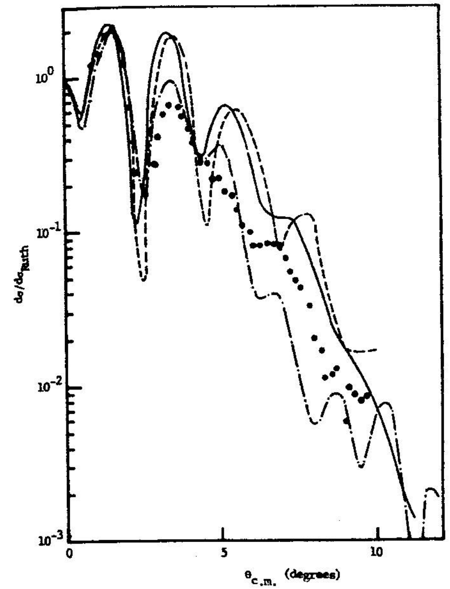

Fig. 11 Same as Fig. 9 but for ^{12}C - ^{12}C at energy 2400 MeV.

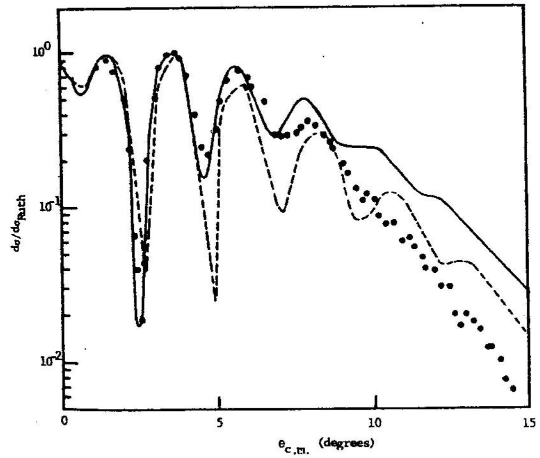

Fig. 12 The elastic scattering differential cross-section of ^{16}O - ^{12}C at 1503 MeV calculated for $\beta_1 = \beta_2 = 60°$ (solid-line) and compared with the results of Lenzi [17] (dashed line).

theoretical calculations. Our results calculated for orientation angles $\beta_1 = \beta_2 = 60°$ are nearly the same as those calculated using the monopole-monopole force of the optical potential and these results agree with the experimental data at the first and second maxima. They give deeper values at the first minimum, but coincide with the second minimum. At angles larger than $\Theta_{c.m} > 6°$, the theoretical calculations are larger than the experimental data. The theoretical results calculated for orientation angles $\beta_1 = \beta_2 = 90°$ are shifted toward smaller angles and that calculated for orientation angles $\beta_1 = \beta_2 = 45°$ are shifted toward larger angles. Fig. 7 is the same as Fig. 5 but for $^{12}C - ^{12}C$ at 2400 MeV. From this figure, we can see that the results calculated using orientation angles $\beta_1 = \beta_2 = 45°, 90°$ do not give the positions of the maxima and the minima. But the theoretical results calculated for $\beta_1 = \beta_2 = 60°$ are nearly the same as those calculated without considering any deformation in the colliding nuclei. We can see that these results give good agreement with experimental data only at the first maximum up to $\Theta_{c.m} > 2.5°$, then they give the same behaviour of experimental data but are of larger values. Fig. 8 is the same as Fig. 5 but for $^{16}O - ^{12}C$ reaction at 1503 MeV. We can see from this figure that our results calculated for $\beta_1 = \beta_2 = 60°$ and those calculated using monopole-monopole force of the optical potential agree with the experimental data up to $\Theta_{c.m} < 9.5°$. At the fourth maximum and beyond it, these theoretical results have larger values than the experimental data. We can see from the above results that our theoretical calculations cannot fit the experimental data at large angles and the inclusion of the excitation to the 2^+ state does not improve the elastic scattering calculation.

Figure 9 shows the comparison of our results calculated for the orientation angles $\beta_1 = \beta_2 = 60°$ compared with the results obtained by Faessler [13] and Lenzi [17] for $^{12}C - ^{12}C$ reaction at energy 1016 MeV. We can see from this figure that the position of the first minimum is obtained accurately by Faessler. The three types of calculations have the same position for the second, third and fourth maxima, but Lenzi could obtain the values of the experimental data at the second maximum only. At the fourth maximum and beyond it, the theoretical calculations are not in agreement with experimental data. Fig. 10 is the same as Fig. 9 but for $^{12}C - ^{12}C$ at 1440 MeV. This figure shows that the three types of results agree with the first experimental maximum. The position of the second maximum is obtained by Lenzi, Ohtsuka and present, but our results agree with the values of the experimental data. At $\Theta_{c.m} \geq 6°$ our results and Faessler results have the same behaviour as that of the experimental data but do not give the proper values of experimental data. The results of Lenzi have a much deeper first and second minima. Fig. 11 is the same as Fig. 9 but for $^{12}C - ^{12}C$ at 2400 MeV. We can see from this figure that the first maximum and minimum are obtained by the three types of calculations. The position of the second maximum is well established by the three types but correspond to larger values than the experimental data. At $\Theta_{c.m} \geq 4°$, the three types of calculations do not reproduce the experimental data. Our results and Lenzi's have larger values than the experimental data and Faessler's results are of smaller values than the experimental data. Fig. 12 shows our calculations for $^{16}O - ^{12}C$ at 1503 MeV which are calculated for orientation angles $\beta_1 = \beta_2 = 60°$ in comparison with the results of Lenzi [17]. We can see from this figure that our calculations agree with the experimental data up to $\Theta_{c.m} \leq 7°$. Lenzi's results do not give the position of the first minimum, and have smaller values at the second and third minimum and the third maximum. At $\Theta_{c.m} \geq 7°$, the two types of calculations could not be in accord with the experimental data. So, from the comparison with the other theoretical calculations, we can see that they cannot give agreement with the experimental data better than

those obtained by our calculations. Changing the orientation angle of scattered nuclei did not improve the agreement with experimental data at large angles but only made a shift to all the distributions.

4. The Reaction Cross-Section

The reaction cross-section is calculated for the reactions under consideration using the equation

$$\sigma_R = \frac{\pi}{k^2} \sum_{l=0}^{\infty} (2l+1)(1 - |S_l|^2),$$

where S_l is given by equation (2.9). The reaction cross-section is calculated at the orientation angles $\beta_1 = \beta_2 = 45°, 60°and90°$. Our results for the reaction cross-section are presented in Table 1 and compared with other results which are measured by the attenuation method [24, 25] and with other theoretical calculations. We can see that our calculations are comparable with the other results, specially the results calculated at the orientation angles $\beta_1 = \beta_2 = 60°$.

5. Conclusion

In this work we study the orientation dependence of the interaction potential between two light deformed nuclei. Also, the orientation dependence is studied for the elastic scattering differential cross-section and the reaction cross-section. These calculation are performed for $^{12}C - ^{12}C$ system at energies 1016, 1440 and 2400 MeV and for $^{16}O - ^{12}C$ system at 1503 MeV. We found that:

1. The optical model potential calculated for deformed nuclei is deeper than that calculated for spherical nuclei. Changing the orientation angle of the deformed nuclei does not affect the depth of the potential, but on increasing the orientation angle, the radius of the potential increases by a very small value and the potential becomes more attractive at large distance (r). Comparing our potential with the potential calculated by Faessler, we can see that our potentials are deeper, but the two potentials have nearly the same radius. The dependence of the double folding potential on the orientation angles of the deformed nuclei was studied by Greiner et al. and they found that rotating the two ^{238}U nuclei produces a dramatic change on the total nucleus-nucleus force at a given r value on nuclear surface. This dramatic change is not expected in our case since we are considering light nuclei with small deformation.

2. On increasing the deformation angles, the angular distribution is shifted towards smaller scattering angles.

3. The reaction cross-section calculated for orientation angles $\beta_1 = \beta_2 = 60°$ is in agreement with the experimental data and with other theoretical calculations.

From the last three points we can see that the orientation and the deformation dependence is not sufficient to obtain a complete agreement with the experimental data and still there is a disagreement at large scattering angles. This implies some modification is needed to obtain a better fit, e.g.

a) Introducing the 3-state of the deformed nuclei.

b) Considering more sophisticated densities for the interacting nuclei such as Woods-Saxon densities and modified Fermi densities and/or another effective nucleon-nucleon interaction such as that of Love and Franey.

References

[1] J.W. Wilson, L.W. Townsend: *Can. J. Phys.* **59** (1981) 1569

[2] J. Wilson: *Phys. Lett.* **B52** (1974) 149

[3] H.B. Bidasaria, L.W. Townsend, J.W. Wilson: *J. Phys.* **G9** (1983) L17

[4] M.C. Mermaz: *Nuovo Cimento* **A88** (1985) 286

[5] M.E. Brandan, G.R. Satchler: *Nucl. Phys.* **A487** (1988) 477

[6] A.M. Kobos et al: *Nucl. Phys.* **A425** (1984) 205 ; L.B. Goldfarm, P. Nagel: *Nucl. Phys.* **A341** (1980) 494 ; A.K. Chaudhuri: *Nucl. Phys.* **A449** (1986) 243 ; A.K. Chaudhuri: *Nucl. Phys.* **A459** (1986) 417

[7] A.M. Kobos, B.A. Brown, P.E. Hodgson, G.R. Satchler, A. Budzanowski: *Nucl. Phys.* **A384** (1982) 65

[8] A.M. Kobos, M.E. Brandan, G.R. Satchler: *Nucl. Phys.* **A487** (1988) 457

[9] P. Roussel et al: *Nucl. Phys.* **A477** (1988) 345

[10] A. Faessler, W.H. Dickfoff, M. Trefz: *Nucl. Phys.* **A428** (1984) 271

[11] M. Trefz, A. Faessler, W.H. Dickhoff, M. Rhoads-Brown: *Phys. Lett.* **B149** (1984) 459

[12] N. Ohtsuka, M. Shabshiry, R. Linden, H. Muther, A. Faessler: *Nucl. Phys.* **A490** (1988) 715

[13] A. Faessler, R. Linden, N Ohtsuka, F.B. Malik: *J.Phys.* **C4** (1986) 111 ; N. Ohtsuka, R. Linder, A. Faessler, F.B. Malik: *Nucl. Phys.* **A465** (1987) 550 ; N. Ohtsuka, R. Linder, A. Faessler: *Phys. Lett.* **B199** (1987) 325

[14] J. Chauvin, D. Lebrum, A. Lounis, M. Buenerd: *Phys. Rev.* **C28** (1983) 1970

[15] P.J. Karol: *Phys. Rev.* **C11** (1975) 1203

[16] G. Faldt, A. Ingemarsson: *Physica Scripta* **28** (1983) 454

[17] S.M. Lenzi, A. Vitturi, F. Zardi: *Phys. Rev.* **C40** (1989) 2114

[18] M.J. Rhoades-Brown, V.E. Aberacker, M. Seiwert, W. Greiner: *Z. Phys.* **A310** (1983) 287

[19] L.W. Townsend, H.B. Bidasaria, J.W. Wilson: *Can. J. Phys.* **61** (1983) 867

[20] O.M. Knyazkov, E.F. Hefter: *Z. Phys.* **A301** (1981) 277

[21] C.W. Dejager, H. Devries, C. Devries: *Atomic data and Nuclear Data Tables* **14** (1974) 479

[22] F.E. Bertrand et al: *Phys. Rev.* **C22** (1980) 1832

[23] P. Roussel et al: *Phys. Rev. Lett.* **54** (1985) 1779

[24] M. Buenerd et al: *Nucl. Phys.* **A424** (1984) 313

[25] J.Y. Hostachy et al: *Phys. Lett.* **B184** (1987) 139